

Extended application of random-walk shielding-potential viscosity model of metals in wide temperature region

Yuqing Cheng

School of Mathematics and Physics, University of Science and Technology Beijing, Beijing 100083, China

Xingyu Gao, Qiong Li, Yu Liu, Haifeng Song, and Haifeng Liu*

Laboratory of Computational Physics, Institute of Applied Physics and Computational Mathematics, Beijing 100094, China

ABSTRACT: The transport properties of matter have been widely investigated. In particular, shear viscosity over a wide parameter space is crucial for various applications, such as designing inertial confinement fusion (ICF) targets and determining the Rayleigh-Taylor instability. In this work, an extended random-walk shielding-potential viscosity model (RWSP-VM) [Phys. Rev. E 106, 014142] based on the statistics of random-walk ions and the Debye shielding effect is proposed to elevate the temperature limit of RWSP-VM in evaluating the shear viscosity of metals. In the extended model, we reconsider the collision diameter that is introduced by hard-sphere concept, hence, it is applicable in both warm and hot temperature regions ($10^1 - 10^7$ eV) rather than the warm temperature region ($10^1 - 10^2$ eV) in which RWSP-VM is applicable. The results of Be, Al, Fe, and U show that the extended model provides a systematic way to calculate the shear viscosity of arbitrary metals at the densities from about 0.1 to 10 times the normal density (the density at room temperature and 1 standard atmosphere). This work will help to develop viscosity model in wide region when combined with our previous low temperature viscosity model [AIP Adv. 11, 015043].

I. INTRODUCTION

Warm and hot matter (WHM) usually refer to the temperature region from several tens of electronvolts (eV) to millions of eV. The transport properties, especially the shear viscosities of WHM are significant in numerous applications, such as designing inertial confinement fusion (ICF) targets [1, 2], determining the Rayleigh-Taylor instability [3, 4], understanding the evolution of astrophysical objects [5, 6], understanding wave damping in dense plasmas [7], microjetting and stability analysis of interface during shock loading [8–10].

Since the experiments of viscosity measurements are very difficult for WHM, researchers have been developing several theoretical methods to obtain demanded viscosity data. For example, first-principles molecular dynamics (FPMD) simulations [11] combined with the Green-Kubo relations [12] are first used by Alfé and Gillan to calculate the viscosity of liquid Al and Fe-S. Hou *et al.* employ both classical molecular dynamics (CMD) and Langevin molecular dynamics (LMD) simulations which are based on average-atom model combined with the hyper-netted chain approximation (AAHNC) to obtain the viscosities of metals (Al, Fe, and U) in warm temperature region [13–15]. The molecular dynamics (MD) simulations are accurate, and the accuracy is ensured by the number of Kohn-Sham orbitals [16] which increase rapidly when the temperature increases. It results in the high cost of MD simulations, which makes it difficult to obtain sufficient amount of data. Therefore, developing more efficient viscosity model is necessary. Stanton-Murillo transport

model (SMT) [17] is based on the Boltzmann equation and employs the Coulomb logarithm to evaluated the momentum-transfer cross section in the Boltzmann equation, and it can be used to calculate the viscosity for high-energy-density matter. The one-component plasma model (OCP) [18] developed by Daligault is based on the equilibrium MD simulations and a practical expression is proposed from the fitting of the MD data to calculate the viscosity of one-component materials from the weakly coupled regime to the solidification threshold. Cléroutin *et al.* extend the Wallenborn-Baus formula [19] by using the data calculated from MD simulations to form an extension of the Wallenborn-Baus fit, and obtain the extended Wallenborn-Baus (EWB) formula, [20] which is applicable to an arbitrary mixture. However, for these models, the parameter space of the MD simulations would limit their applicable region. Therefore, in a previous work [14], we developed an analytical model called “random-walk shielding-potential viscosity model” (RWSP-VM) to evaluate the shear viscosity. It is based on the statistics of random-walk ions and the Debye shielding effect. Compared with the models and the simulation methods mentioned above, it is applicable in warm temperature region (several tens of eV to hundreds of eV), and it has the advantages of universality, accuracy, and efficiency.

In this work, we extend RWSP-VM by reconsidering the collision distance which is introduced by the hard-sphere concept. This new model named as ext-RWSP-VM has a wider temperature range of applications, i.e., it is not only applicable in warm temperature region, but also in hot temperature region (hundreds of eV to millions of eV), maintaining the advantages of RWSP-VM simultaneously.

* Corresponding author: liu_haifeng@iapcm.ac.cn

II. MODEL

As the temperature increases, the ionization of the metal increases. Particularly, in warm temperature region, electrons are partially ionized; while in hot temperature region, most or all of the electrons are ionized. It results in the fact that the metal ions are principally influenced by the Coulomb interactions between each other. The interactions led to the motion variation of the ions, which can be treated as a kind of “collisions”, which is called as the Coulomb collisions or distant collisions due to the long range nature of the Coulomb potential. On the other hand, in both regions, the ion velocities are high enough that they can be treated as “ion gas” which move randomly, so that the concept of random-walk can process their behaviours properly. Moreover, the Debye shielding effect plays an important role, and the real interactions among these ions are the shielding Coulomb potential, which can be processed by considering the Coulomb potential with a cutoff distance r_0 , i.e., the Coulomb potential works only if $r < r_0$. Therefore, the main part of the track of the ions is hyperbola, as shown in Fig. 1. Here, the hyperbolic equation is $\frac{x^2}{a^2} - \frac{y^2}{b^2} = 1$, where a is the semimajor axis and b is the semiminor axis, with the focal length $c = \sqrt{a^2 + b^2}$. The viscosity η is evaluated by the formula below [14]:

$$\eta = \frac{\sqrt{3mk_B T}}{\pi d^4} I. \quad (1)$$

Here m is the atom mass, k_B is the Boltzmann constant, T is the temperature, d is the collision diameter introduced by hard-sphere concept, and I is a quantity that is relevant to T , which can be expressed as:

$$I = 2r_0^2 \frac{K [2(1-K) + (1+K)\ln K]}{(1+\sqrt{K})^2(1-K)^2}. \quad (2)$$

Here, $K = \left(\frac{r_0 - a}{a}\right)^2$, $a = \frac{q^2}{3k_B T + 2q^2/r_0}$, $q^2 = \frac{(\bar{Z}e)^2}{4\pi\epsilon_0}$, $\bar{Z} = \frac{1}{n} \sum_{j=0}^Z j n_j$ is the average ionization, Z is the nuclear charge, n_j is the number density of the j th ionized ion, and r_0 is the cutoff distance which is introduced by the Debye shielding effect. In RWSP-VM, we assumed that both d and r_0 equal to the Debye length $\lambda_D \equiv \sqrt{\frac{\epsilon_0 k_B T}{n_e e^2 (z^* + 1)}}$, where $z^* \equiv \bar{Z}^2 / \bar{Z}$ and $\bar{Z}^2 = \frac{1}{n} \sum_{j=0}^Z j^2 n_j$. The approximation $d = \lambda_D$ is successful in warm temperature region. However, in hot temperature region, the large λ_D and the almost full-ionization both make the ions interact more strongly; moreover, the speed of the ions are so large that the collision distance is much smaller than the cutoff distance, resulting in the failure of $d = \lambda_D$, thus the inapplicability of RWSP-VM. Because r_0 and d represent the maximum and the minimum distances between two ions within interaction, respectively, and the higher T is, the smaller d is; while λ_D increases with the increasing T . When T

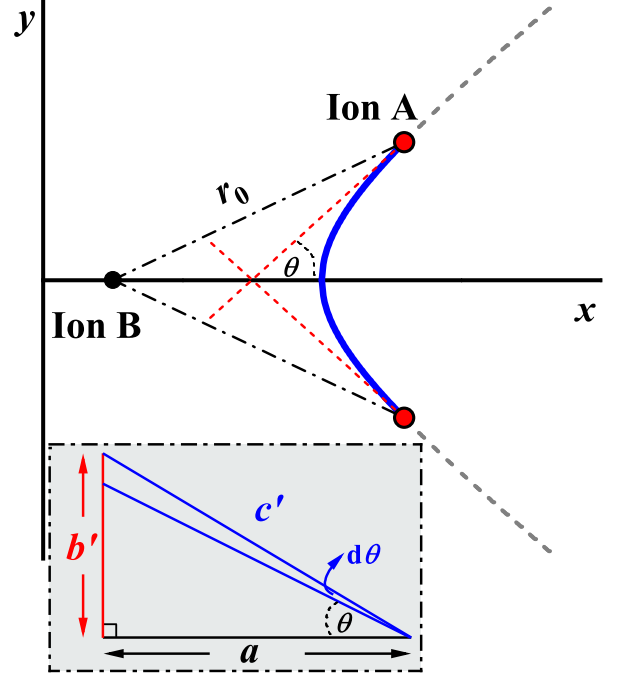


FIG. 1. Schematic of the track of the ions. r_0 is the cutoff distance, i.e., there is interaction between the two ions only when the separation distance r is smaller than r_0 . Blue solid curve represents the hyperbolic track. θ is the incident angle between the incident velocity and x -axis. The inset is the scheme of the integration over θ , where $b' = \frac{R}{\sqrt{R^2 - c^2}} b$ and $c' = \sqrt{\frac{R^2 - a^2}{R^2 - c^2}} c$. Here $R \equiv r_0 - a$.

is high, d is much smaller than λ_D , resulting in the fact that $d \neq \lambda_D$. Therefore, the limit of RWSP-VM is that it is applied only in warm temperature region though it has good characteristics such as universality, accuracy, and high efficiency. In this work, we extend it to hot temperature region by carefully reconsidering d analytically, i.e., calculating its average value over scattering angles of the collisions between ions. The extended model is called ext-RWSP-VM.

Here, the assumption that the cutoff distance is equal to the Debye length is still a good approximation:

$$r_0 = \lambda_D. \quad (3)$$

However, we should carefully reconsider d . The track of the ions is hyperbola, as shown in Fig. 1. The minimum distance between two ions should be $(a + c)$. For certain temperature T , a is determined, but b varies with the scattering angles of the collisions, resulting in the varying c . Therefore, we calculate the average value of d over

incident angles:

$$d = \overline{a+c} = \frac{\int_0^{\theta_m} (a+c) \sin \theta \, d\theta}{\int_0^{\theta_m} \sin \theta \, d\theta} \quad (4)$$

$$= a \left[1 + \frac{R}{b_m} \ln \left(\frac{R+b_m}{a} \right) \right].$$

Here, $\theta_m = \pi/2$, $\sin \theta = b'/c' = R/\sqrt{R^2 - a^2}$, and $b_m = \sqrt{r_0^2 - 2r_0 a}$. The relationships among these parameters are displayed in Ref. [14] and can be interpreted in the inset of Fig. 1, e.g., b ranges from 0 to b_m which results in b' ranging from 0 to $+\infty$ and θ ranging from 0 to $\pi/2$. Combining Eqs. 1-4, we obtain the analytical expressions of the shear viscosity for ext-RWSP-VM. We have compared several methods which calculate \bar{Z} (Thomas-Fermi (TF) model [21, 22], density functional theory MD [23], path integral Monte Carlo approach [24], AAHNC approximation [25], and the Hartree-Fock-Slater model [26], etc.) in Ref. [14], and concluded that all of these methods agree well with each other with certain differences in warm and hot temperature regions. Due to the simplicity, efficiency, and accuracy of TF model [21, 22], we choose it to calculate the average ionization \bar{Z} .

III. RESULTS AND DISCUSSIONS

First, we take Al as an example to illustrate the validity of ext-RWSP-VM. Fig. 2 shows the shear viscosity of Al at the densities of 2.7 and 27 g/cm³. The results of ext-RWSP-VM are compared with the ones of RWSP-VM [14], SMT [17], OCP [18], EWB [20], and LMD [13]. Here, the applicable region of each model is clarified in their articles. SMT is applicable for $\Gamma < 10$, $\Gamma < 20$, and $\Gamma < 100$ for $\kappa = 1$, $\kappa = 2$, and $\kappa = 3$, respectively. The expression of OCP is applicable for $\Gamma < 200$ in the case of $\kappa = 0$. EWB is applicable for $\Gamma < 160$. Here, $\Gamma = q^2/(a_{ws} k_B T)$ is the coupling parameter, $a_{ws} = (\frac{3}{4\pi n})^{1/3}$ is the Wigner-Seitz radius of the ion, and κ is the screening parameter.

In warm temperature region (about 10-500 eV) and at the densities of both 2.7 and 27 g/cm³, ext-RWSP-VM agrees well with RWSP-VM, and the former is slightly larger than the latter. Both of them agree well with OCP and CMD. In hot temperature region (about over 500 eV) and at the densities of both 2.7 and 27 g/cm³, RWSP-VM fails, but ext-RWSP-VM agrees well with SMT and EWB, with a certain difference. At the density of 8.1 g/cm³, the phenomenon (which is not shown in Fig. 2) is almost similar to the ones of 2.7 and 27 g/cm³. It can be concluded that ext-RWSP-VM is applicable in warm and hot temperature regions, i.e., T satisfies $\lambda_D(T) > 0.1 a_{ws}$ [14]. In the approximation of $z^* + 1 \approx \bar{Z}$ for large \bar{Z} , the relation can be easily reduced to $\Gamma < 100/3 \approx 33.3$. In other words, the lower temperature limit is estimated T_{lower} by $\Gamma(T_{\text{lower}}) \approx 33.3$. On the other hand, the upper

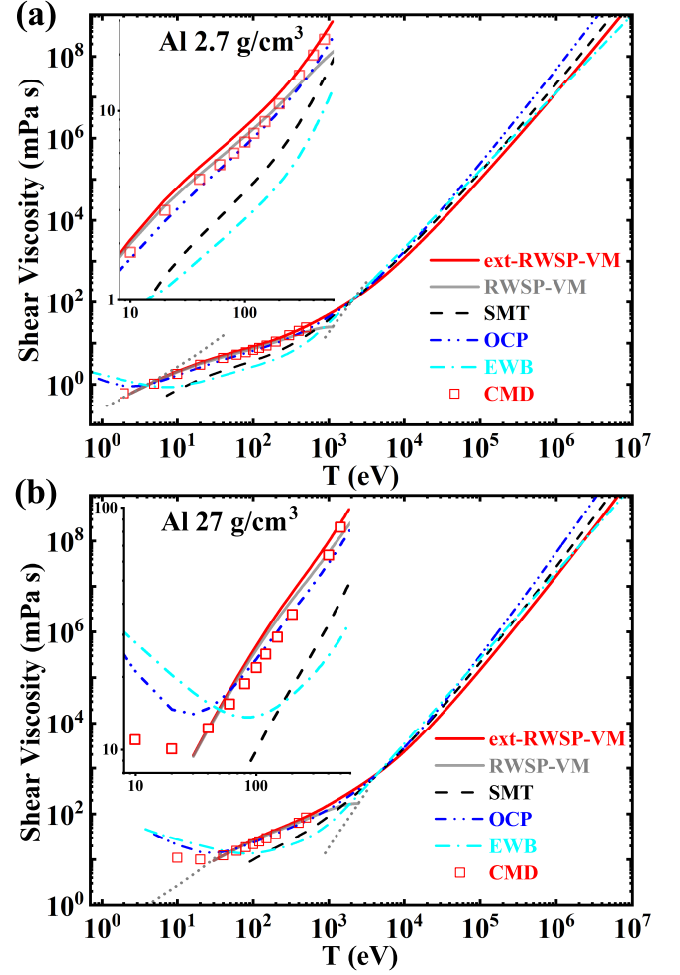


FIG. 2. Shear viscosity of Al at the density of 2.7 g/cm³ (a) and 27 g/cm³ (b). Red solid, gray solid, black dashed, blue dash-dot-dot, and cyan dash-dot curves stand for the results of ext-RWSP-VM, RWSP-VM [14], SMT [17], OCP [18], and EWB [20], respectively. Open squares stand for the results of CMD [13]. The gray dotted lines represent the lower (left) and upper (right) limits of the warm temperature region in which RWSP-VM is applicable. Each inset stands for the zoom of temperature from about $T = 10$ eV to $T = 600$ eV.

temperature limit of ext-RWSP-VM should be within the nonrelativistic approximation ($T_{\text{upper}} \approx 10^7$ eV), i.e., it doesn't contain the relativistic temperature region. This model indicates that as the temperature or/and the density increases, the viscosity increases.

Second, in addition to Al, we take several other elements, i.e., Be, Fe, and U, as examples to show the results of ext-RWSP-VM, as shown in Fig. 3, Fig. 4, and Fig. 5, respectively. The results calculated from ext-RWSP-VM are compared with the ones of RWSP-VM and the MD simulations. In general, for all these metals ext-RWSP-VM agrees well with RWSP-VM in warm temperature region; for Be, Al, and Fe, ext-RWSP-VM agrees well with CMD, but for U, ext-RWSP-VM agrees well with CMD at lower density (1.893 g/cm³) and

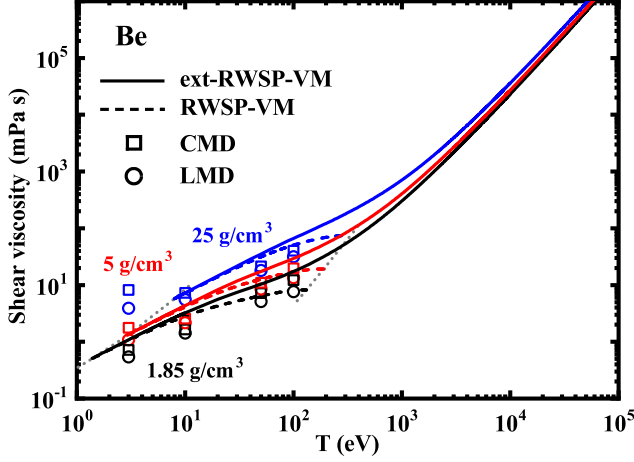


FIG. 3. Shear viscosity of Be. Solid curves, dashed curves, open squares, and open circles stand for ext-RWSP-VM, RWSP-VM, CMD, and LMD [14], respectively. Black, red, and blue stand for the densities of 1.85, 5.0, and 25 g/cm³, respectively. The gray dotted lines represent the lower (left) and upper (right) limits of the warm temperature region in which RWSP-VM is applicable.

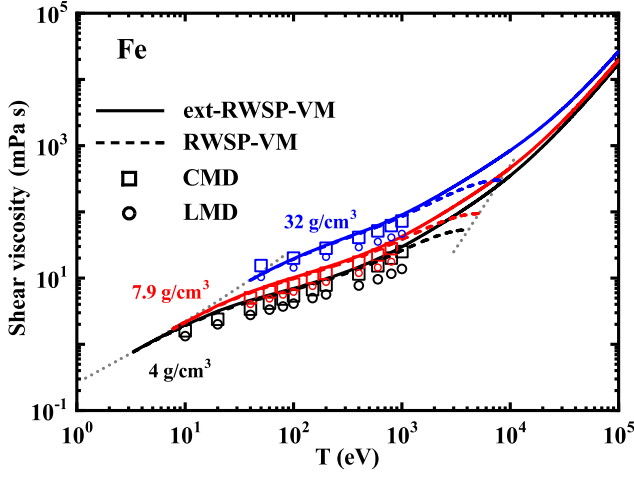


FIG. 4. Shear viscosity of Fe. Solid curves, dashed curves, open squares, and open circles stand for ext-RWSP-VM, RWSP-VM, CMD, and LMD [14], respectively. Black, red, and blue stand for the densities of 4.0, 7.9, and 32 g/cm³, respectively. The gray dotted lines represent the lower (left) and upper (right) limits of the warm temperature region in which RWSP-VM is applicable.

with Langevin MD simulations (LMD) at higher density (94.65 g/cm³), the derivations of which have already been discussed in RWSP-VM [14]. Here, we summarize in brief that at higher densities, the interaction between ions are weakened by the nonadiabatic dynamic effects. Because for high-Z elements at higher densities, the ionic structures are complex with the increase temperature. In this case,

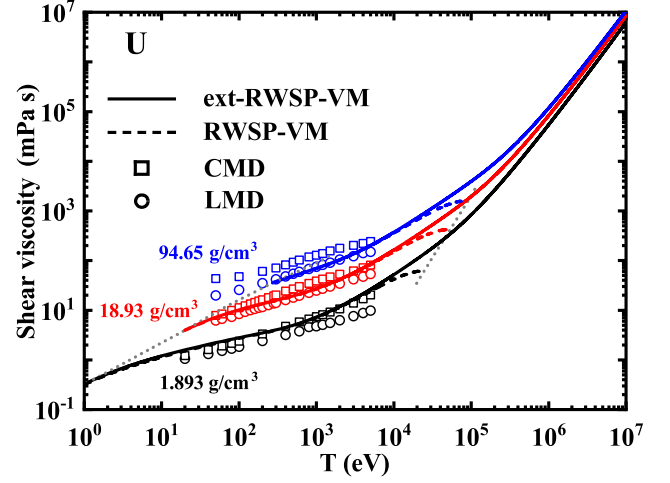


FIG. 5. Shear viscosity of U. Solid curves, dashed curves, open squares, and open circles stand for ext-RWSP-VM, RWSP-VM, CMD, and LMD [15], respectively. Black, red, and blue stand for the densities of 1.893, 18.93, and 94.65 g/cm³, respectively. The gray dotted lines represent the lower (left) and upper (right) limits of the warm temperature region in which RWSP-VM is applicable.

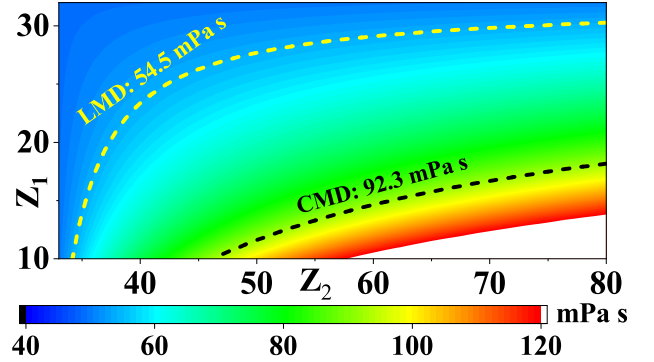


FIG. 6. Shear viscosity of U varying with Z_1 and Z_2 at the density of 94.65 g/cm³ and $T = 500$ eV. The yellow and black dashed curves stand for the contour lines of 54.5 mPa s (LMD) and 92.3 mPa s (CMD), respectively. The unit of the color bar is mPa s.

LMD is more appropriate than CMD due to the fact that LMD considers interaction between ions and electrons, which corresponds to the Debye shielding effect in our model.

As mentioned above, for high-Z elements such as U, the ionizations are complicated at higher densities. Here, we give a detailed derivation for the complex ionization case to calculate the viscosities. Notice two important facts. First, $z^* = \bar{Z}$ is not a good approximate, i.e., $z^* > \bar{Z}$, which may influence the value of the viscosities. Second, we cannot approximately treat all the ions charged with \bar{Z} to calculate the term I that is relevant to the hyperbolic track. We are recalling that n_j is the

number density of the j th ionized ions, thus $x_j = n_j/n$ the proportion. Therefore, to calculate the contribution of the j th ionized ions, we define:

$$q_j^2 = \frac{e^2}{4\pi\epsilon_0} \sum_{k=1}^Z j \cdot k \cdot x_k = \frac{e^2}{4\pi\epsilon_0} j \bar{Z}. \quad (5)$$

All other quantities relevant to q_j^2 should be recalculated, e.g., a_j , R_j , K_j , b_{mj} , I_j , and d_j , except for $r_0 = \lambda_D$ (z^* should follow its definition strictly). Therefore, the total viscosity should be contributed by all the ionized ions:

$$\eta = \sum_{j=1}^Z \eta_j = \sum_{j=1}^Z x_j \frac{\sqrt{3mk_B T}}{\pi d_j^4} I_j. \quad (6)$$

We take the two-ionization situation of U at the density of 94.65 g/cm³ and at the temperature of 500 eV as an example. Based on TF model and ext-RWSP-VM, the average ionization is $\bar{Z} = 32.8$ and the viscosity is $\eta = 49.1$ mPa s. Assume that there are only two ionizations for the ions, i.e., Z_1 and Z_2 , respectively ($Z_1 < \bar{Z}$ and $Z_2 > \bar{Z}$). Therefore, we have the equations $x_{z1}Z_1 + x_{z2}Z_2 = \bar{Z}$ and $x_{z1} + x_{z2} = 1$ to obtain x_{z1} and x_{z2} . Using Eqs. 5 and 6, we can obtain the viscosity varying with Z_1 and Z_2 , as shown in Fig. 6. It is obvious that when Z_1 decreases or/and Z_2 increases, i.e., they are far away from \bar{Z} , the viscosity increases. As a result, the ionization distributions influence the values of the shear viscosities based on ext-RWSP-VM. Although the ionization distributions are complicated for high-Z elements, the results of ext-RWSP-VM using only \bar{Z} ionization as the approximation agree well with the ones of LMD that considers the complication of the ionizations, which indicates the validity of ext-RWSP-VM, as shown in Fig. 5.

From the above elaborations, we can conclude that ext-RWSP-VM is accurate for arbitrary metal and is

applicable in both warm and hot temperature regions, and in certain density region.

CONCLUSIONS

In conclusion, we show that RWSP-VM can be extended to hot temperature region with a satisfactory accuracy when the collision distance is appropriately reconsidered. The improvement of ext-RWSP-VM is that it implements unified modeling in both warm and hot temperature regions (10¹ – 10⁷ eV), and at the densities from about 0.1 to 10 times the normal density (the density at room temperature and 1 standard atmosphere). Moreover, as with RWSP-VM, ext-RWSP-VM is also universal, accurate, and efficient. It is helpful to the development of unified viscosity model in wide region.

The data and the codes which support the findings of this study are available from the corresponding author upon reasonable request.

ACKNOWLEDGMENT

This work was supported by Laboratory of Computational Physics (Grant No. 6142A05220303).

DISCLOSURES

The authors declare no conflicts of interest.

REFERENCES

-
- [1] Lindl, J.; Landen, O.; Edwards, J.; Moses, E.; Team, N. Review of the National Ignition Campaign 2009-2012. *Physics of Plasmas* **2014**, *21*, 020501.
 - [2] Regan, S. et al. The National Direct-Drive Inertial Confinement Fusion Program. *Nuclear Fusion* **2018**, *59*, 032007.
 - [3] Sauppe, J. P.; Palaniyappan, S.; Loomis, E. N.; Kline, J. L.; Flippo, K. A.; Srinivasan, B. Using cylindrical implosions to investigate hydrodynamic instabilities in convergent geometry. *Matter and Radiation at Extremes* **2019**, *4*, 065403.
 - [4] Terasaki, H.; Sakaiya, T.; Shigemori, K.; Akimoto, K.; Kato, H.; Hironaka, Y.; Kondo, T. In situ observation of the Rayleigh-Taylor instability of liquid Fe and Fe-Si alloys under extreme conditions: Implications for planetary core formation. *Matter and Radiation at Extremes* **2021**, *6*, 054403.
 - [5] Duffy, T. S.; Smith, R. F. Ultra-High Pressure Dynamic Compression of Geological Materials. *Frontiers in Earth Science* **2019**, *7*, 23.
 - [6] Bruno, D.; Catalfamo, C.; Capitelli, M.; Colonna, G.; De Pascale, O.; Diomede, P.; Gorse, C.; Laricchiuta, A.; Longo, S.; Giordano, D.; Pirani, F. Transport properties of high-temperature Jupiter atmosphere components. *Physics of Plasmas* **2010**, *17*, 112315.
 - [7] Wong, A. Y.; Motley, R. W.; D'Angelo, N. Landau Damping of Ion Acoustic Waves in Highly Ionized Plasmas. *Physical Review* **1964**, *133*, A436–A442.
 - [8] Durand, O.; Jaouen, S.; Soulard, L.; Heuzé, O.; Colombet, L. Comparative simulations of microjetting using atomistic and continuous approaches in the presence of viscosity and surface tension. *Journal of Applied Physics* **2017**, *122*, 135107.
 - [9] Pei, L.; Ma, Z.; Zhang, Y.; Shi, X.; Ma, D.; Pan, H.; Wang, P. Discrete element simulations on the damaged

- surface hydrodynamics of tungsten powders with inert Ar gas. *Journal of Applied Physics* **2022**, *131*, 025901.
- [10] Yin, J.-W.; Pan, H.; Wu, Z.-H.; Hao, P.-C.; Duan, Z.-P.; Xiao-Mian, H. Stability analysis of interfacial Richtmyer-Meshkov flow of explosion-driven copper interface. *Acta Physica Sinica* **2017**, *66*, 204701.
- [11] Alfè, D.; Gillan, M. J. First-Principles Calculation of Transport Coefficients. *Physical Review Letters* **1998**, *81*, 5161–5164.
- [12] Allen, M. P.; Tildesley, D. J. *Computer Simulation of Liquids*; Clarendon Press, 1989.
- [13] Hou, Y.; Fu, Y.; Bredow, R.; Kang, D.; Redmer, R.; Yuan, J. Average-atom model for two-temperature states and ionic transport properties of aluminum in the warm dense matter regime. *High Energy Density Physics* **2017**, *22*, 21–26.
- [14] Cheng, Y.; Liu, H.; Hou, Y.; Meng, X.; Li, Q.; Liu, Y.; Gao, X.; Yuan, J.; Song, H.; Wang, J. Random-walk shielding-potential viscosity model for warm dense metals. *Physical Review E* **2022**, *106*, 014142.
- [15] Hou, Y.; Jin, Y.; Zhang, P.; Kang, D.; Gao, C.; Redmer, R.; Yuan, J. Ionic self-diffusion coefficient and shear viscosity of high-Z materials in the hot dense regime. *Matter and Radiation at Extremes* **2021**, *6*, 026901.
- [16] Blanchet, A.; Torrent, M.; Clérouin, J. Requirements for very high temperature Kohn–Sham DFT simulations and how to bypass them. *Physics of Plasmas* **2020**, *27*, 122706.
- [17] Stanton, L. G.; Murillo, M. S. Ionic transport in high-energy-density matter. *Physical Review E* **2016**, *93*, 043203.
- [18] Daligault, J.; Rasmussen, K. Ø.; Baalrud, S. D. Determination of the shear viscosity of the one-component plasma. *Physical Review E* **2014**, *90*, 033105.
- [19] Wallenborn, J.; Baus, M. Kinetic theory of the shear viscosity of a strongly coupled classical one-component plasma. *Physical Review A* **1978**, *18*, 1737–1747.
- [20] Clérouin, J. G.; Cherfi, M. H.; Zérah, G. The viscosity of dense plasmas mixtures. *Europhysics Letters* **1998**, *42*, 37.
- [21] Thomas, L. H. The calculation of atomic fields. *Mathematical Proceedings of the Cambridge Philosophical Society* **1927**, *23*, 542–548.
- [22] More, R. Pressure Ionization, Resonances, and the Continuity of Bound and Free States. **1985**, *21*, 305–356.
- [23] Bethkenhagen, M.; Witte, B. B. L.; Schörner, M.; Röpke, G.; Döppner, T.; Kraus, D.; Glenzer, S. H.; Sterne, P. A.; Redmer, R. Carbon ionization at gigabar pressures: An ab initio perspective on astrophysical high-density plasmas. *Physical Review Research* **2020**, *2*, 023260.
- [24] Driver, K. P.; Soubiran, F.; Militzer, B. Path integral Monte Carlo simulations of warm dense aluminum. *Physical Review E* **2018**, *97*, 063207.
- [25] Fu, Y.; Hou, Y.; Kang, D.; Gao, C.; Jin, F.; Yuan, J. Multi-charge-state molecular dynamics and self-diffusion coefficient in the warm dense matter regime. *Physics of Plasmas* **2018**, *25*, 012701.
- [26] Meng, X.-J.; Sun, Y.-S.; Li, S.-C. Calculation of atomic average degree of ionization. *Acta Physica Sinica* **1994**, *43*, 345–350.